Glass transition in systems without static correlations: a microscopic theory

2003 J. Phys.: Condens. Matter 15 S967

(http://iopscience.iop.org/0953-8984/15/11/320)

INSTITUTE OF PHYSICS PUBLISHING JOURNAL OF PHYSICS: CONDENSED MATTER

J. Phys.: Condens. Matter **15** (2003) S967–S985 PII: S0953-8984(03)57930-9

Glass transition in systems without static correlations: a microscopic theory

R Schilling[1] **and G Szamel**[1,2]

[1] Institut für Physik, Johannes Gutenberg-Universität Mainz, D-55099 Mainz, Germany
[2] Department of Chemistry, Colorado State University, Ft. Collins, CO 80523, USA

Received 27 September 2002
Published 10 March 2003
Online at stacks.iop.org/JPhysCM/15/S967

Abstract

We present a first step toward a microscopic theory for the glass transition in systems with trivial static correlations. As an example we have chosen N infinitely thin hard rods with length L, fixed with their centres on a periodic lattice with lattice constant a. Starting from the N-rod Smoluchowski equation we derive a coupled set of equations for fluctuations of reduced k-rod densities. We approximate the influence of the surrounding rods on the dynamics of a pair of rods by introduction of an effective rotational diffusion tensor $\boldsymbol{D}(\Omega_1, \Omega_2)$ and in this way we obtain a self-consistent equation for $\boldsymbol{D}$. This equation exhibits a feedback mechanism leading to a slowing down of the relaxation. It involves as an input the Laplace transform $\upsilon_0(l/r)$ at $z = 0$, $l = L/a$, of a torque–torque correlator of an isolated pair of rods with distance $R = ar$. Our equation predicts the existence of a continuous ergodicity-breaking transition at a critical length $l_c = L_c/a$. To estimate the critical length we perform an approximate analytical calculation of $\upsilon_0(l/r)$ based on a variational approach and obtain $l_c^{\mathrm{var}} \cong 5.68$, 4.84 and 3.96 for an sc, bcc and fcc lattice. We also evaluate $\upsilon_0(l/r)$ numerically exactly from a two-rod simulation. The latter calculation leads to $l_c^{\mathrm{num}} \cong 3.45$, 2.78 and 2.20 for the corresponding lattices. Close to l_c the rotational diffusion constant decreases as $D(l) \sim (l_c - l)^{\gamma}$ with $\gamma = 1$ and a diverging timescale $t_\epsilon \sim |l_c - l|^{-\delta}$, $\delta = 2$, appears. On this timescale the t- and l-dependence of the one-rod density is determined by a master function depending only on t/t_ϵ. In contrast to present microscopic theories our approach predicts a glass transition despite the absence of any static correlations.

1. Introduction

In the last two decades huge theoretical efforts were made in order to describe the glass transition on a *microscopic* level in systems *without* quenched disorder. Microscopic means that, e.g., the glass transition temperature and the dynamical properties in its vicinity can be calculated from

equations which use as an input the knowledge of the interactions between microscopic constituents of the system (atoms or molecules; hereafter we use the term particles). Most of this activity has been devoted to *structural glasses* [1–4]. Although experiments [5–8] have demonstrated that plastic crystals can exhibit an *orientational* glass transition which has many features in common with the structural glass transition there seems to be no analytical theory for such systems[3]. On the other hand molecular dynamics (MD) simulations [11–13] have confirmed the similarity between glassy behaviour of plastic crystals and that of supercooled liquids.

The first successful microscopic theoretical approach to glassy dynamics in supercooled liquids came from so-called mode coupling theory (MCT) [1, 2]. This theory was first suggested and mainly worked out in detail by Götze and his co-workers. For reviews the reader may consult [14–16]. MCT derives a closed set of equations for time-dependent correlators, like the intermediate scattering function $S(q, t)$. This set uses as an input the corresponding *static* correlations, e.g. $S(q)$, which depend only on thermodynamic variables like temperature T, density n etc. The static correlations can be calculated from the microscopic interactions by use of either analytical or numerical tools [17]. By decreasing T (or increasing n) the peaks of $S(q)$ grow. If their magnitude becomes large enough a transition from an ergodic to a non-ergodic phase occurs at a critical temperature T_c (or density n_c). This *dynamic* transition is interpreted as an ideal glass transition. MCT makes several non-trivial predictions for, e.g., time dependence of correlators [14–16] which have been successfully tested (see [18–21] for reviews).

The second microscopic theory of the glass transition has been developed by Mézard and Parisi [3]. Their first principles theory combines the use of the replica idea known from the spin glass theory and of the liquid state theory techniques. It is related to an earlier density functional approach [4]. The theory of Mézard and Parisi starts from the microscopic Hamiltonian for m identical replicas of the system to which a symmetry breaking field is added. The free energy of the replicated system is then calculated and the configurational entropy of the original system is extracted from it. The theory predicts the existence of a critical temperature T_f (which is below T_c of MCT) at which the configurational entropy vanishes. This is then interpreted as an ideal *static* glass transition.

Besides these two microscopic theories, let us mention one other attempt to describe the glass transition that does not resort to microscopic potentials: based on several *qualitative* assumptions Edwards and Vilgis [22] obtained the dependence of the self-diffusion constant D for a system of hard rods on physical control parameter x, e.g., concentration, diameter or length of the rods. A dynamical glass transition occurs when D becomes zero. A mean field treatment results in $D \sim x_c - x$ and an improved approach leads to the Vogel–Fulcher law $D \sim \exp[A/(x_c - x)]$. Close to the critical point x_c a power law dependence of D on $(x_c - x)$ is found with a non-trivial exponent $\gamma = 7/6$.

Both the above described microscopic theories have at least one feature in common: non-trivial equilibrium correlations. These correlations are of primary importance for both theories. For example, MCT requires that the vertices which enter into the self-consistent equations for the correlation functions must depend on at least one control parameter. Recently, it has been shown that a colloidal suspension with hard core plus attractive Yukawa potential can undergo a gel transition [23] in a special limit: $\phi \to 0$ and $K \to \infty$ such that $\Gamma = K^2\phi/b =$ constant. Here ϕ is the volume fraction, K the interaction strength and b a measure of the inverse range of interaction. In that limit the direct correlation function $c(q)$ is proportional to K and becomes independent of ϕ [24]. This implies that the static correlations vanish, i.e. $S(q) \to 1$. But

[3] The microscopic theory developed by Michel and Bostoen [9, 10] is valid for the orientational glass transition of mixed crystals, i.e. crystals with *quenched* disorder.

since the vertices are proportional to ϕ and involve a bilinear product of $c(q)$ they become proportional to Γ. Accordingly, despite the vanishing of the static correlations there is still an ergodicity breaking transition driven by the increase of Γ [23–25]. Of course, this type of behaviour is not generic in the ϕ–K phase space. In addition, whether the mode coupling approximation remains reasonable must be still checked.

One may now ask the following question: can there be a *generic* glass transition if and only if there exist non-trivial static correlations? To find an answer let us consider a liquid of hard rods. This system was used as a paradigm in [22]. If the rod thickness d is finite the static correlations are non-trivial and a glass transition will be predicted by either theory. However, in the limit of *infinitely thin* hard rods, i.e. $d = 0$, with *finite* length L and *finite* concentration c, the static properties become trivial. Note that in this limit there is no transition to a nematic phase. Also, according to either of the two microscopic theories there is no glass transition! In the case of MCT the vertices vanish. The absence of a glass transition is also consistent with a microscopic theory worked out by one of the present authors and his co-workers [26, 27]. There, it was shown that for infinitely thin hard rods with randomly frozen orientations translational diffusion never ceases if the diffusion constant along the rod's direction is non-zero.

Now suppose we fix the infinitely thin hard rods with their centres on the sites of a three-dimensional periodic lattice. Such a model has already been suggested earlier [22, 28]. It can be used to describe the steric hindrance of the orientational degrees of freedom in plastic crystals [6–8, 11–13]. Again, both MCT and the replica theory exclude a glass transition, due to the lack of static correlations. The fact that MCT in its present form does not predict a glass transition has already been stressed in [29]. Nevertheless, computer simulations [29, 30] showed glassy behaviour and suggested a *dynamical* ergodicity-breaking transition at a critical length[4] L_c. This simple example makes it clear that non-trivial static behaviour is *not* necessary for a glass transition. It is the main goal of our paper to present a microscopic approach to the glass transition for systems without static correlations.

A short account of our approach for the case of a simple cubic lattice was given in [31]. In the present paper we will discuss our model and the theoretical framework in more detail and will extend the results to bcc and fcc lattices. Furthermore, we will investigate the type of glass transition and the long time dynamics in its vicinity.

The outline of our paper is as follows. In the next section we will present and discuss the model. The third section contains the analytical theory used to describe the glass transition. The results are given in the fourth section and the final section includes a summary and some conclusions.

2. Model

We consider N hard, infinitely thin rods (i.e. diameter $d = 0$) with length L and with their centres fixed at the lattice sites of a *periodic* lattice with lattice constant a. The dimensionless control parameter is the reduced rod length, $l = L/a$. In the following we will restrict ourselves to a simple cubic lattice. Its unit cell is depicted in figure 1. All qualitative conclusions which will be drawn in this paper remain valid for *all* periodic lattices.

It is obvious that for $l \leqslant 1$ each rod can rotate freely: there is no steric hindrance. For l above one, collisions between a rod and adjacent ones appear. If $1 \leqslant l \leqslant \sqrt{2}$ a given rod interacts only with the six nearest neighbours. Further increase of l will introduce collisions

[4] Note that different cubic lattices were used in [29] and [30]; moreover the authors of [30] fixed the rods with one of their endpoints at the lattice sites.

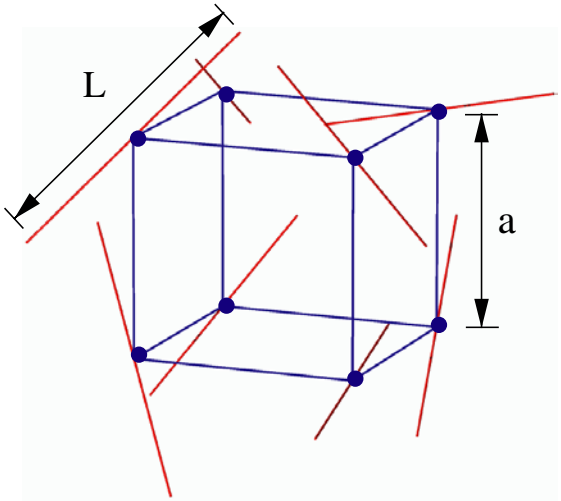

Figure 1. Unit cell of the sc lattice with lattice constant a with hard rods of length L. (This figure is in colour only in the electronic version)

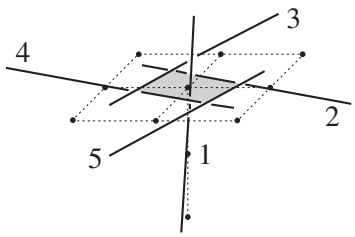

Figure 2. Illustration of the blocking of rod 1 by rods 2–5 within shaded region for $l > 2$.

between next-, third-, fourth- etc nearest neighbours, generating a strong increase of steric hindrance. Since we have chosen infinitely thin rods there is no equilibrium transition to an orientationally ordered phase. On the other hand, due to the rise of steric hindrance with l we expect an orientational glass transition as detected in [29] and [30]. Although steric hindrance already exists for $l > 1$, it seems that no ergodicity-breaking transition can occur for $l < 2$. Let us consider the following simple argument. If $l > 2$ then the nearest-neighbour rods of a tagged rod (rod 1) can 'overlap' with, e.g., the top of the tagged rod (see figure 2). This induces a 'cage' for the tagged rod. Note that this argument is not rigorous, because for $l < 2$ there might exist other configurations similar to the one shown in figure 2 which could block the tagged rod's rotation. But the value $l = 2$ also plays a role from a different point of view. Consider two neighbouring rods with their centres along the z-axis. Their orientations can be described by $\Omega_i = (\theta_i, \phi_i)$ and $\Omega_j = (\theta_j, \phi_j)$. At a collision we have either $\phi_j = \phi_i^{\pm}$ (see figure 3(a)) or $\phi_j = \phi_i^{\pm} + \pi$ (see figure 3(b)), for fixed θ_i, θ_j and ϕ_i. The notation ϕ_i^{+} and ϕ_i^{-} means that rod j is behind and in front of rod i, respectively (see figure 3). Now, it is easy to prove that for *arbitrary* θ_i and θ_j there exists only *one* contact (either at $\phi_i^{\pm}$ *or* at $\phi_i^{\pm} + \pi$) for $l < 2$ (see figures 3(a), (b)). In that case ϕ_j can be varied freely by 2π. But for $l > 2$ there is a finite range for both angles θ_i and θ_j such that *two* contacts (at $\phi_i^{\pm}$ *and* $\phi_i^{\pm} + \pi$) exist (see figure 3(c)). Therefore the 'phase space' $[0, 2\pi]$ for $\phi_j - \phi_i$ is decomposed into two 'ergodic' components $[0, \pi]$ and $[\pi, 2\pi]$ for θ_i and θ_j kept fixed. Transitions between both components

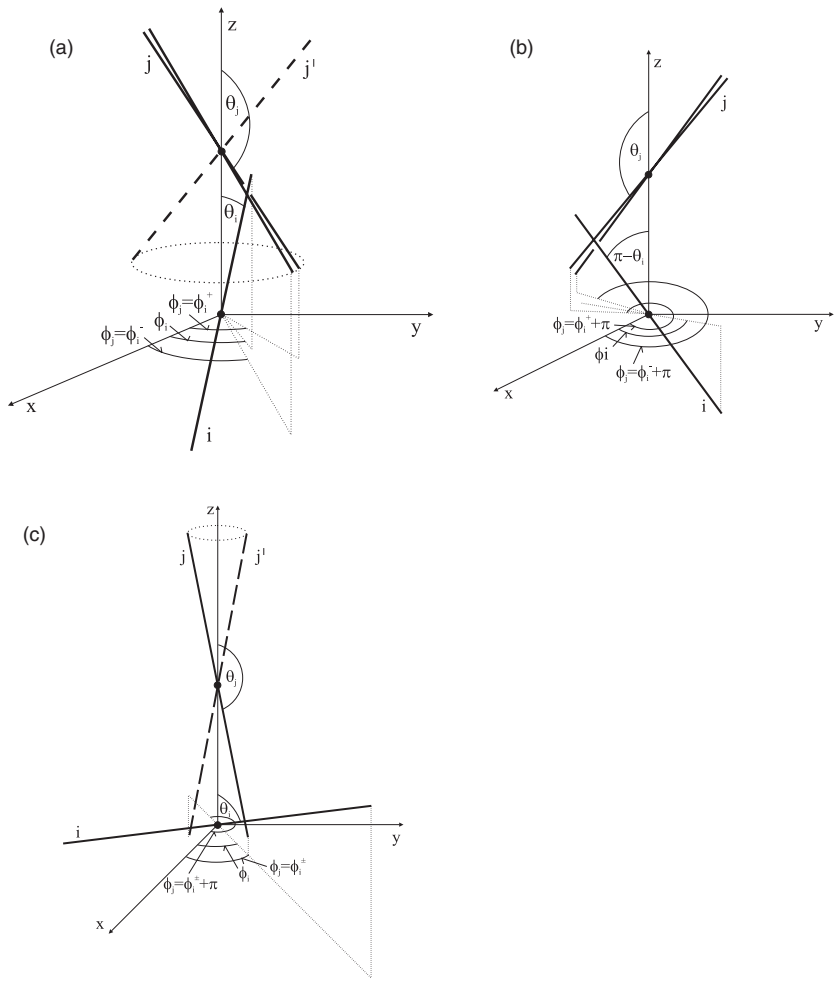

Figure 3. Illustration of possible collisions of rod i and j for fixed rod i. For better visualization a small but finite thickness has been used. (a) Single collision for $l < 2$ at $\phi_j = \phi_i^{\pm}$. The rod j' (dashed) turned around the z-axis by π does not lead to a second collision if $l < 2$. (b) Single collision for $l < 2$ at $\phi_j = \phi_i^{\pm} + \pi$. Again a rotation by π (not shown) does not yield a second collision (c) Two collisions for $l > 2$; θ_i and θ_j are chosen such that two collisions occur at $\phi_j = \phi_i^{\pm}$ and $\phi_j = \phi_i^{\pm} + \pi$.

are forbidden. If the rods are fixed at the lattice sites with one of their end points (as in [30]) then there is only one contact, for *all* $l > 1/2$.

The condition for a collision can be quantified as follows [32]. Let $\boldsymbol{u}_i$ and $\boldsymbol{u}_j$ be the unit vectors along rod i and j and $\boldsymbol{r}_{ij}$ the vector connecting the centre of rod j with that of rod i (see figure 4). $\boldsymbol{u}_i$ and $\boldsymbol{u}_j$ define a plane. Let $\boldsymbol{r}_{ij}^{\perp}$ be the component of $\boldsymbol{r}_{ij}$ perpendicular to that plane and $r_{ij}^{\perp} = |\boldsymbol{r}_{ij}^{\perp}|$. Denote the distance of the point of contact to the centre of rod i and j by, respectively, s_{ij} and s_{ji} (figure 4). Then a collision occurs if

$$r_{ij}^{\perp} = 0^{+}, \qquad |s_{ij}| < L/2, \qquad |s_{ji}| < L/2 \tag{1}$$

where 0^{+} represents the limit $d \to 0$. Simple algebra yields

$$s_{ij} = -[(\boldsymbol{u}_i \cdot \boldsymbol{r}_{ij}) - (\boldsymbol{u}_i \cdot \boldsymbol{u}_j)(\boldsymbol{u}_j \cdot \boldsymbol{r}_{ij})]/[1 - (\boldsymbol{u}_i \cdot \boldsymbol{u}_j)^2] \tag{2}$$

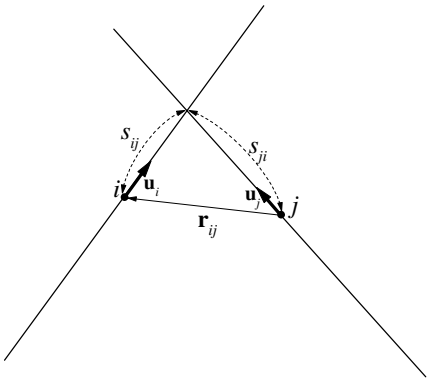

Figure 4. Illustration of geometrical quantities defined in the text for two rods i and j.

$$s_{ji} = [(\boldsymbol{u}_j \cdot \boldsymbol{r}_{ij}) - (\boldsymbol{u}_i \cdot \boldsymbol{u}_j)(\boldsymbol{u}_i \cdot \boldsymbol{r}_{ij})]/[1 - (\boldsymbol{u}_i \cdot \boldsymbol{u}_j)^2]. \tag{3}$$

Note

(i) that s_{ij} and s_{ji} can be negative; in that case the contact points into the direction of $-\boldsymbol{u}_i$ and $-\boldsymbol{u}_j$, respectively, and
(ii) that $\boldsymbol{r}_{ij}$ is time independent and is always equal to a lattice vector $\boldsymbol{R}_{ij} = \boldsymbol{R}_i - \boldsymbol{R}_j$.

The configurational part of the partition function is given by

$$Z_c(T, N; l) = \int \prod_{i=1}^{N} \mathrm{d}\Omega_i \, \mathrm{e}^{-\beta V(\Omega_1, \ldots, \Omega_N)} = (4\pi)^N, \qquad \beta = (k_B T)^{-1} \tag{4}$$

since the hard rod interaction potential $V(\Omega_1, \ldots, \Omega_N)$ vanishes almost everywhere. The corresponding contribution $-k_B T N \ln 4\pi$ to the free energy is analytic in temperature T and does not depend on l. Hence, there is no equilibrium phase transition. The equilibrium pair distribution function $g_{ij}^{(2)}(\Omega_i, \Omega_j)$ is related to the probability of finding a rod at $\boldsymbol{R}_i$ and $\boldsymbol{R}_j (\neq \boldsymbol{R}_i)$ with orientations Ω_i and Ω_j, respectively. It is given by

$$g_{ij}^{(2)}(\Omega_i, \Omega_j) = 1 - \theta\big(0^+ - r_{ij}^{\perp}\big)\theta\left(\frac{L}{2} - |s_{ij}|\right)\theta\left(\frac{L}{2} - |s_{ji}|\right) \tag{5}$$

where the Heaviside functions are non-zero at a collision, which happens if conditions (1) are fulfilled. Since a collision is non-generic, $g_{ij}^{(2)}(\Omega_i, \Omega_j) = 1$ for almost all Ω_i and Ω_j. Hence there are no static correlations, except on a set of measure zero.

3. Kinetic theory

In this section we will describe the dynamics for our model and the approximations leading to a closed set of equations. We assume that the microscopic N-rod dynamics of the system is Brownian rather than Newtonian. Previous studies of systems with non-trivial static correlations have indicated that glassy dynamics should not depend on that choice [33, 34].

The starting point of the theory is the so-called generalized Smoluchowski equation for the N-rod probability density $P_N(\Omega_1, \ldots, \Omega_N; t)$ [32],

$$\frac{\partial}{\partial t} P_N(\Omega_1, \ldots, \Omega_N; t) = D_0 \sum_{n=1}^{N} \nabla_n \cdot [\nabla_n - \boldsymbol{T}_n(\Omega_1, \ldots, \Omega_N)] P_N(\Omega_1, \ldots, \Omega_N; t) \tag{6}$$

where D_0 is the *bare* rotational diffusion constant, $\nabla_n \equiv \nabla_{\Omega_n} \equiv \boldsymbol{u}_n \times \nabla_{\boldsymbol{u}_n}$ and

$$\boldsymbol{T}_n(\Omega_1, \ldots, \Omega_N) = \sum_{j \neq n} \boldsymbol{T}_{jn}(\Omega_j, \Omega_n). \tag{7}$$

$\boldsymbol{T}_{ij}(\Omega_i, \Omega_j)$ describes the singular torque when two rods at sites i and j with vector distance $\boldsymbol{r}_{ij}$ collide:

$$\boldsymbol{T}_{ij}(\Omega_i, \Omega_j) = s_{ij}(\boldsymbol{u}_i \times \hat{\boldsymbol{r}}_{ij}^{\perp})\delta(r_{ij}^{\perp} - 0^+)\theta\left(\frac{L}{2} - |s_{ij}|\right)\theta\left(\frac{L}{2} - |s_{ji}|\right) \tag{8}$$

where $\hat{\boldsymbol{r}}_{ij}^{\perp} = \boldsymbol{r}_{ij}^{\perp}/r_{ij}^{\perp}$. Using equation (5) it is easy to prove that

$$\nabla_i g_{ij}^{(2)}(\Omega_i, \Omega_j) = \boldsymbol{T}_{ij}(\Omega_i, \Omega_j) g_{ij}^{(2)}(\Omega_i, \Omega_j). \tag{9}$$

Equation (9) describes the non-crossability condition. Note that $\boldsymbol{T}_{ij}(\Omega_i, \Omega_j)$ differs slightly from $\boldsymbol{T}_{ij}(\Omega_i, \Omega_j)$ used in [32] since there ∇_{u_i} was used instead of ∇_{Ω_i}. Also, a similar generalized Smoluchowski equation had been used before to describe a liquid of infinitely thin hard rods with randomly frozen orientations [26, 27].

In a next step we present equations of motion for the reduced k-rod density

$$\rho_{n_1 \cdots n_k}^{(k)}(\Omega_1, \ldots, \Omega_k; t) = \int \prod_{n \neq n_1, \ldots, n_k} \mathrm{d}\Omega_n \, P_N(\Omega_1, \ldots, \Omega_N; t). \tag{10}$$

These equations form an infinite, coupled hierarchy [35] of the following form:

$$\frac{\partial}{\partial t} \rho_{n_1 \cdots n_k}^{(k)}(\Omega_1, \ldots, \Omega_k; t) = \mathcal{L}^{(k)} \rho_{n_1 \cdots n_k}^{(k)}(\Omega_1, \ldots, \Omega_k; t)$$
$$- D_0 \sum_{n \in I_k} \sum_{n_{k+1} \notin I_k} \nabla_n \cdot \int \mathrm{d}\Omega_{k+1} \, \boldsymbol{T}_{n n_{k+1}}(\Omega_n, \Omega_{k+1}) \rho_{n_1 \cdots n_{k+1}}^{(k+1)}(\Omega_1, \ldots, \Omega_{k+1}; t) \tag{11}$$

with the k-rod Smoluchowski operator,

$$\mathcal{L}^{(k)} = D_0 \sum_{n \in I_k} \nabla_n \cdot \left[\nabla_n - \sum_{\substack{n' \in I_k \\ n' (\neq n)}} \boldsymbol{T}_{n n'}(\Omega_n, \Omega_{n'}) \right] \tag{12}$$

and $I_k = \{n_1, \ldots, n_k\}$. As initial conditions we choose

$$\rho_{n_1 \cdots n_k}^{(k)}(\Omega_1, \ldots, \Omega_k; 0) = \frac{1}{(4\pi)^{k-1}} \delta(\Omega_1 | \Omega_0) g_{n_1 \cdots n_k}^{(k)}(\Omega_1, \ldots, \Omega_k), \tag{13}$$

where $\delta(\Omega|\Omega') = \sin\theta \delta(\theta - \theta')\delta(\phi - \phi')$. Here, $g_{n_1 \cdots n_k}^{(k)}(\Omega_1, \ldots, \Omega_k)$ is the equilibrium k-rod distribution function which is equal to one almost everywhere.

To proceed we introduce the fluctuations of the k-rod density for $k \geqslant 2$

$$\delta\rho_{n_1 \cdots n_k}^{(k)}(\Omega_1, \ldots, \Omega_k; t) = \rho_{n_1 \cdots n_k}^{(k)}(\Omega_1, \ldots, \Omega_k; t) - \frac{1}{(4\pi)^{k-1}} g_{n_1 \cdots n_k}^{(k)}(\Omega_1, \ldots, \Omega_k) \rho_{n_1}^{(1)}(\Omega_1; t). \tag{14}$$

These fluctuations vanish in equilibrium and for $t = 0$.

Substituting $\rho^{(k)}$ from equation (14) into (11) and taking into account that the equilibrium k-rod rotational current density vanishes we obtain the following equation:

$$\frac{\partial}{\partial t} \rho_{n_1}^{(1)}(\Omega_1; t) + \nabla_1 \cdot \boldsymbol{j}_{n_1}^{(1)}(\Omega_1; t) = 0 \tag{15}$$

where the one-rod rotational current density reads

$$\boldsymbol{j}_{n_1}^{(1)}(\Omega_1; t) = -D_0 \left\{ \nabla_1 \rho_{n_1}^{(1)}(\Omega_1; t) - \sum_{n_2 \neq n_1} \int \mathrm{d}\Omega_2 \, \boldsymbol{T}_{n_1 n_2}(\Omega_1, \Omega_2) \delta\rho_{n_1 n_2}^{(2)}(\Omega_1, \Omega_2; t) \right\}. \tag{16}$$

At the next level, $k = 2$, it follows by use of equation (9) that

$$\frac{\partial}{\partial t}\delta\rho^{(2)}_{n_1n_2}(\Omega_1,\Omega_2;t) = -\frac{1}{4\pi}\boldsymbol{T}_{n_1,n_2}(\Omega_1,\Omega_2)g^{(2)}_{n_1n_2}(\Omega_1,\Omega_2)\cdot\boldsymbol{j}^{(1)}_{n_1}(\Omega_1;t)$$
$$+ D_0\{\nabla_1\cdot[\nabla_1 - \boldsymbol{T}_{n_1n_2}(\Omega_1,\Omega_2)] + (1\leftrightarrow 2)\}\delta\rho^{(2)}_{n_1n_2}(\Omega_1,\Omega_2;t)$$
$$+ A^{(2)}_{n_1n_2}(\Omega_1,\Omega_2;t) \tag{17}$$

where

$$A^{(2)}_{n_1n_2}(\Omega_1,\Omega_2;t) = D_0\nabla_1\cdot\left[g^{(2)}_{n_1n_2}(\Omega_1,\Omega_2)\sum_{n_3}\frac{1}{4\pi}\int \mathrm{d}\Omega_3\,\boldsymbol{T}_{n_1n_3}(\Omega_1,\Omega_3)\delta\rho^{(2)}_{n_1n_3}(\Omega_1,\Omega_3;t)\right]$$
$$- D_0\sum_{\nu=1}^{2}\nabla_\nu\cdot\sum_{n_3}\int \mathrm{d}\Omega_3\,\boldsymbol{T}_{n_\nu n_3}(\Omega_\nu,\Omega_3)\delta\rho^{(3)}_{n_1n_2n_3}(\Omega_1,\Omega_2,\Omega_3;t). \tag{18}$$

Let us interpret these equations: equation (15) is the continuity equation. The corresponding one-rod current density (equation (16)) consists of two parts. The first describes the contribution from the free Brownian dynamics of a tagged rod at site n_1 and the second is due to the interaction of the tagged rod with a second rod at side n_2. The first line on the rhs of equation (17) originates from the last term on the rhs of equation (14); its second line describes Brownian dynamics of an *isolated* pair of rods at sites n_1 and n_2 and the last line contains the influence of a third rod at n_3 on the rods at n_1 and n_2. In order to close this set of equations we follow the strategy of [26, 27] and approximate the influence of a third rod by introducing an effective, non-local (in angular space and time) diffusion tensor $\boldsymbol{D}^{\mathrm{eff}}(\Omega,\Omega';t)$ and simultaneously neglecting $A^{(2)}_{n_1n_2}$:

$$\{D_0\nabla_1\cdot[\nabla_1 - \boldsymbol{T}_{n_1n_2}(\Omega_1,\Omega_2)] + (1\leftrightarrow 2)\}\delta\rho^{(2)}_{n_1n_2}(\Omega_1,\Omega_2;t)$$
$$\to\left\{\nabla_1\cdot\int_0^t \mathrm{d}t'\int \mathrm{d}\Omega_1'\,\boldsymbol{D}^{\mathrm{eff}}(\Omega_1,\Omega_1';t-t')\cdot[\nabla_1' - \boldsymbol{T}_{n_1n_2}(\Omega_1',\Omega_2)]\right.$$
$$\times\,\delta\rho^{(2)}_{n_1n_2}(\Omega_1',\Omega_2;t) + \nabla_2\cdot\int_0^t \mathrm{d}t'\int \mathrm{d}\Omega_2'\,\boldsymbol{D}^{\mathrm{eff}}(\Omega_2,\Omega_2';t-t')$$
$$\left.\times\,[\nabla_2' - \boldsymbol{T}_{n_2n_1}(\Omega_2',\Omega_1)]\delta\rho^{(2)}_{n_1n_2}(\Omega_1,\Omega_2';t)\right\}$$
$$=: (\Lambda^{(2)} * \delta\rho^{(2)})_{n_1n_2}(\Omega_1,\Omega_2;t), \tag{19}$$
$$A^{(2)}_{n_1n_2}(\Omega_1,\Omega_2;t)\approx 0. \tag{20}$$

The generalized rotational diffusion tensor $\boldsymbol{D}(\Omega,\Omega';t)$ is defined through a constitutive equation relating the one-rod current density and the (angular) gradient of the one-rod density

$$\boldsymbol{j}^{(1)}_{n_1}(\Omega;t) = -\int_0^t \mathrm{d}t'\int \mathrm{d}\Omega'\,\boldsymbol{D}(\Omega,\Omega';t-t')\cdot\nabla_{\Omega'}\rho^{(1)}_{n_1}(\Omega';t). \tag{21}$$

As the final approximation we impose a self-consistency condition,

$$\boldsymbol{D}^{\mathrm{eff}} = \boldsymbol{D}. \tag{22}$$

Equations (15)–(17) and (19)–(22) form a closed set of equations for $\rho^{(1)}$, $\delta\rho^{(2)}$ and $\boldsymbol{D}$. Taking their Laplace transform[5] it is straightforward to (formally) eliminate $\rho^{(1)}$ and $\delta\rho^{(2)}$ which results in:

[5] Here we use the definition $\hat{f}(z) = \int_0^\infty \mathrm{d}t\, f(t)\exp(-zt)$, $\mathrm{Re}\, z > 0$ and take $\delta\rho^{(2)}_{n_1n_2}(\Omega_1,\Omega_2;t=0) = 0$ into account.

$$D_0^{-1}\hat{\boldsymbol{j}}_{n_1}(\Omega_1; z) + \sum_{n_3}\frac{1}{4\pi}\int \mathrm{d}\Omega_3\, \boldsymbol{T}_{n_1n_3}(\Omega_1, \Omega_3)[(z - \hat{\Lambda}^{(2)})^{-1} * (\boldsymbol{T}_{n_1n_3}g^{(2)}_{n_1n_3} \cdot \hat{\boldsymbol{j}}^{(1)}_{n_1})]_{n_1n_3}(\Omega_1, \Omega_3; z) = \int \mathrm{d}\Omega_3\, \hat{\boldsymbol{D}}^{-1}(\Omega_1, \Omega_3; z) \cdot \hat{\boldsymbol{j}}_{n_1}(\Omega_3; z) \tag{23}$$

where $\hat{}$ denotes the Laplace transformed quantities. From equation (23) we find immediately the self-consistent equation for $\hat{\boldsymbol{D}}(\Omega_1, \Omega_2; z)$:

$$\hat{\boldsymbol{D}}^{-1}(\Omega_1, \Omega_2; z) = \boldsymbol{D}_0^{-1}\delta(\Omega_1|\Omega_2) + \frac{1}{4\pi}\sum_{n_3}\boldsymbol{T}_{n_1n_3}(\Omega_1, \Omega_2)[(z - \hat{\Lambda}^{(2)})^{-1} * (\boldsymbol{T}^t_{n_1n_3}g^{(2)}_{n_1n_3})]_{n_1n_3}(\Omega_1, \Omega_2; z). \tag{24}$$

Taking the limit $z \to 0$ in equation (24) and operating with $(1/4\pi)\int \mathrm{d}\Omega_1 \int \mathrm{d}\Omega_2$ on both sides of the resulting equation yields the following for the diffusion tensor $\boldsymbol{D}(\Omega_1, \Omega_2) \equiv \hat{\boldsymbol{D}}(\Omega_1, \Omega_2; z = 0)$:

$$4\pi\langle \boldsymbol{D}^{-1}\rangle = \boldsymbol{D}_0^{-1} - \sum_{n_3}\langle(\hat{\Lambda}^{(2)\dagger})^{-1} * \boldsymbol{T})_{n_1n_3}\boldsymbol{T}^t_{n_1n_3}\rangle \tag{25}$$

with

$$\langle f_{n_1n_2}\, h_{n_1n_2}\rangle = \frac{1}{(4\pi)^2}\int \mathrm{d}\Omega_1 \int \mathrm{d}\Omega_2\, g^{(2)}_{n_1n_2}(\Omega_1, \Omega_2) f^*_{n_1n_2}(\Omega_1, \Omega_2) h_{n_1n_2}(\Omega_1, \Omega_2), \tag{26}$$

and

$$(\boldsymbol{D}_0)^{\alpha\beta} = D_0\delta^{\alpha\beta}. \tag{27}$$

$\boldsymbol{T}^t$ is the transpose of $\boldsymbol{T}$ and for the adjoint two-rod operator we find from equation (19)

$$(\hat{\Lambda}^{(2)\dagger} * f)_{n_1n_2}(\Omega_1, \Omega_2) = [\nabla_1 + \boldsymbol{T}_{n_1n_2}(\Omega_1, \Omega_2)] \cdot \int \mathrm{d}\Omega_3\, \boldsymbol{D}(\Omega_3, \Omega_1) \cdot \nabla_3 f_{n_1n_2}(\Omega_3, \Omega_2) + [\nabla_2 + \boldsymbol{T}_{n_2n_1}(\Omega_2, \Omega_1)] \cdot \int \mathrm{d}\Omega_3\, \boldsymbol{D}(\Omega_3, \Omega_2) \cdot \nabla_3 f_{n_1n_2}(\Omega_1, \Omega_3). \tag{28}$$

The reader should note that

(i) $g^{(2)}_{n_1n_2}(\Omega_1, \Omega_2)$ in equation (26) can be skipped, because it is equal to one almost everywhere; of course, it must not be dropped if ∇_1 or ∇_2 act on it, as in equation (18); in that case one can use equation (9);
(ii) $\langle \boldsymbol{D}^{-1}\rangle$ does not depend on n_1 and n_2 and
(iii) the tensor $\langle((\hat{\Lambda}^{(2)\dagger})^{-1} * \boldsymbol{T})_{n_1n_3}\boldsymbol{T}^t_{n_1n_3}\rangle$ in equation (25) depends only on $\boldsymbol{R}_{n_3} - \boldsymbol{R}_{n_1}$ because of the lattice translational invariance.

Accordingly $\sum_{n_3}\langle\cdots\rangle$ does not depend on n_1. Equation (25) can also be rewritten as follows:

$$4\pi\langle \boldsymbol{D}^{-1}\rangle = \boldsymbol{D}_0^{-1} + \sum_{n_3}\int_0^\infty \mathrm{d}t\,\langle(\mathrm{e}^{\hat{\Lambda}^{(2)\dagger}t} * \boldsymbol{T})_{n_1n_3}\boldsymbol{T}^t_{n_1n_3}\rangle. \tag{29}$$

Let us discuss equation (29). It is a *functional equation* for the rotational diffusion tensor $\boldsymbol{D}$, since $\hat{\Lambda}^{(2)\dagger}$ also involves $\boldsymbol{D}$. If $l \leqslant 1$ then $\boldsymbol{T}_{n_1n_2}(\Omega_1, \Omega_2) \equiv 0$ and therefore equation (29) implies that

$$\boldsymbol{D}(\Omega_1, \Omega_2) = \boldsymbol{D}_0\delta(\Omega_1|\Omega_2) \tag{30}$$

as it should. Increasing l beyond one leads to an 'increase' of the friction tensor $\langle \boldsymbol{D}^{-1}\rangle$, due to the positive definite, time-dependent torque–torque correlation tensor $\langle(\exp(\hat{\Lambda}^{(2)\dagger}t) *$

$\boldsymbol{T})_{n_1n_3}\boldsymbol{T}^t_{n_1n_3}\rangle$ which determines the second term in equation (29). This 'increase' of the 'renormalized' friction tensor $\boldsymbol{D}^{-1}$ implies a decrease of the 'renormalized' diffusion tensor $\boldsymbol{D}$. Since this one enters the exponent of $\exp(\hat{\Lambda}^{(2)\dagger}t)$ the relaxation of the torque–torque correlation will slow down. This in turn leads to an 'increase' of the second term of equation (29) leading to a further 'increase' of $\boldsymbol{D}^{-1}$ and so on. This feedback mechanism, which is different from but still resembles that of MCT [14–16], may finally lead to the vanishing of diffusion and therefore to a glass transition.

Although the functional equation possesses a rather clear structure it probably cannot be solved exactly. For this one would have to determine the eigenvalues and eigenfunctions of $\hat{\Lambda}^{(2)\dagger}$. Due to the singular character of $\boldsymbol{T}_{n_1n_2}(\Omega_1, \Omega_2)$ (cf equation (8)) on the three-dimensional contact hypersurface defined by equation (1) this does not seem to be feasible. In order to make progress and to get explicit results for $\boldsymbol{D}$ we will use the following additional approximation:

$$(\boldsymbol{D}(\Omega_1, \Omega_2))^{\alpha\beta} \approx D(l)\delta^{\alpha\beta}\delta(\Omega_1|\Omega_2). \tag{31}$$

Substituting equation (31) into (29) and acting with $\frac{1}{3}\sum_{\alpha,\beta}$ on both sides yields

$$D(l) = D_0[1 - \upsilon(l)]. \tag{32}$$

The l-dependent coupling function $\upsilon(l)$ follows from the second term of equation (29) by use of equations (28) and (31):

$$\upsilon(l) = \tfrac{1}{3}\sum_{n_3}\int_0^\infty \mathrm{d}t\, \langle \boldsymbol{T}_{n_1n_3} \cdot \mathrm{e}^{\mathcal{L}^{(2)\dagger}t}\boldsymbol{T}_{n_1n_3}\rangle \tag{33}$$

with the adjoint of the two-rod Smoluchowski operator (cf equation (12)),

$$\mathcal{L}^{(2)\dagger} = [\nabla_1 + \boldsymbol{T}_{n_1n_2}(\Omega_1, \Omega_2)] \cdot \nabla_1 + (1 \leftrightarrow 2) \tag{34}$$

where D_0 is replaced by one. The calculation of the relevant quantity $\upsilon(l)$ and the determination of a critical length l_c at which $D(l)$ vanishes will be presented in the next section.

4. Results

4.1. Glass transition singularity

Using the local approximation equation (31), we obtained equation (32) which constitutes a rather simple result. Before we calculate $\upsilon(l)$ let us discuss $D(l)$ and $\upsilon(l)$ on a qualitative level. Since $\boldsymbol{T}_{n_1n_2}(\Omega_1, \Omega_2) \equiv 0$ for $l \leqslant 1$ it follows that $\upsilon(l) = 0$ and therefore $D(l) = D_0$ for $l \leqslant 1$, as it should. Next, we introduce

$$\upsilon_0(l/r_n) = \tfrac{1}{3}\int_0^\infty \mathrm{d}t\, \langle \boldsymbol{T}_{0n} \cdot \mathrm{e}^{\mathcal{L}^{(2)\dagger}t}\, \boldsymbol{T}_{0n}\rangle \tag{35}$$

where $r_n = |\boldsymbol{R}_n|/a$. This is related to the torque–torque correlator of one rod at the origin and another one at site n. Note that the rhs of equation (35) depends on $|\boldsymbol{R}_n|$, but not on the direction of $\boldsymbol{R}_n$. $\upsilon_0(x)$, of course, vanishes for $x \leqslant 1$, is positive for $x > 1$ (see below) and we expect it to converge to a finite limit υ_0^∞ for $x \to \infty$. $\upsilon(l)$ is completely determined by $\upsilon_0(x)$:

$$\upsilon(l) = \sum_n \upsilon_0(l/r_n) \tag{36}$$

where the sum is restricted to such n for which $r_n < l$. This relation can be used to determine the asymptotic behaviour of $\upsilon(l)$ for $l \to \infty$. Approximating the sum by an integral which becomes more and more accurate with increasing r_n we get

$$\upsilon(l) \approx \int_{1\leqslant r\leqslant l} \mathrm{d}^3 r\, \upsilon_0(l/r) = 4\pi \int_1^l \mathrm{d}r\, r^2 \upsilon_0(l/r) = 4\pi \left(\int_{l^{-1}}^1 \mathrm{d}x\, x^2 \upsilon_0\left(\frac{1}{x}\right)\right) l^3$$

which gives

$$\upsilon(l) \approx c \cdot l^3 + \mathrm{O}(l^2), \qquad l \to \infty \tag{37}$$

with

$$c = 4\pi \int_0^1 \mathrm{d}x\, x^2 \upsilon_0\left(\frac{1}{x}\right) > 0. \tag{38}$$

That $\upsilon(l) \sim l^3$ for $l \to \infty$ is obvious since all rods within a sphere of radius of order l will collide with the central one. Their number, of course, is proportional to l^3. Because $\upsilon(l) = 0$ for $l \leqslant 1$ and $\upsilon(l)$ increases linearly with l^3 for large l there must exist a critical length l_c for which $\upsilon(l_c) = 1$ and therefore $D(l_c) = 0$. To determine l_c at which a dynamical glass transition takes place we have to calculate $\upsilon_0(x)$. Although this quantity is much simpler than the second term in equation (29), it cannot be determined exactly analytically (see below). Therefore the exact evaluation can only be done numerically. For such a numerically exact calculation we performed a simulation of the Brownian dynamics (defined by $\mathcal{L}^{(2)\dagger}$) of an *isolated* pair of rods with distance r_n. The time-dependent torque–torque correlator resulting from this simulation is shown in figure 5 for several values of l/r_n. For $t \to 0$ we find a power law divergence $t^{-1/2}$ as expected and already proven for the force–force correlator of hard spheres [36, 37]. Since only two rods are considered, the system is ergodic and therefore the torque correlations relax to zero. Figure 5 shows that the relaxational behaviour changes qualitatively around $l/r_n = 2$ from a fast decay as for free Brownian dynamics to a rather slow relaxation. This crossover at $l/r_n \approx 2$ is related to the properties discussed in section 2. Whether the *long-time* decay of the torque–torque correlation is purely exponential, proportional to $t^{-\alpha}\exp(-\lambda t)$ or even a single power law $t^{-\alpha}$ (as is true for two hard spheres [36]) cannot be decided from our numerical data. Although the log–linear representation in figure 5 exhibits a bending for large t (which would indicate deviation from a pure exponential) the exponential behaviour could appear on a much larger timescale on which the statistical fluctuations of the numerical data prevent the determination of the precise long-time decay. The numerical evaluation of the time integral in equation (35) leads to $\upsilon_0^{\mathrm{num}}(x)$ presented in figure 6. The reader should note the strong increase starting at $x = l/r_n \approx 2$.

Now let us turn to the analytical calculation of $\upsilon_0(x)$. For this we rewrite $\upsilon_0(x)$ as

$$\upsilon_0(x) = \tfrac{1}{3}\langle \boldsymbol{T}_{0n} \cdot (-\mathcal{L}^{(2)\dagger})^{-1} \boldsymbol{T}_{0n}\rangle \tag{39}$$

which is (up to the factor $1/3$) the Laplace transformed torque–torque correlator at $z = 0$.

Analogous to [26, 27] we introduce a vector function $\boldsymbol{f}_{n_1n_2}(\Omega_1, \Omega_2)$ such that

$$\mathcal{L}^{(2)\dagger} \boldsymbol{f}_{n_1n_2}(\Omega_1, \Omega_2) = \boldsymbol{T}_{n_1n_2}(\Omega_1, \Omega_2). \tag{40}$$

Equation (40) can be decomposed into a *regular* part

$$[\nabla_1^2 + \nabla_2^2]\boldsymbol{f}_{n_1n_2}(\Omega_1, \Omega_2) = 0, \tag{41}$$

and a singular one

$$[s_{12}(\boldsymbol{u}_1 \times \hat{\boldsymbol{r}}_{12}^{\perp}) \cdot \boldsymbol{\nabla}_1 + s_{21}(\boldsymbol{u}_2 \times \hat{\boldsymbol{r}}_{21}^{\perp}) \cdot \boldsymbol{\nabla}_2]\boldsymbol{f}_{n_1n_2}(\Omega_1, \Omega_2) = s_{12}(\boldsymbol{u}_1 \times \hat{\boldsymbol{r}}_{12}^{\perp}). \tag{42}$$

Equation (42) is to be satisfied for Ω_1, Ω_2 located on the three-dimensional contact hypersurface. Accordingly, equations (41) and (42) describe a boundary value problem with boundary value on the three-dimensional hypersurface embedded in the four-dimensional space built by the surface of two unit spheres. This is a difficult mathematical problem which seems

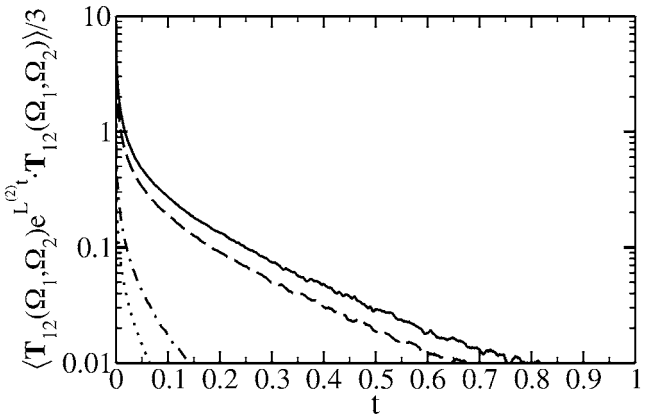

Figure 5. Time dependence of the torque–torque correlator of an isolated pair of rods for different l/r_n. Dotted curve, $l/r_n = 1.8$; dash–dotted curve, $l/r_n = 2$; dashed curve, $l/r_n = 4$; solid curve, $l/r_n = 6$.

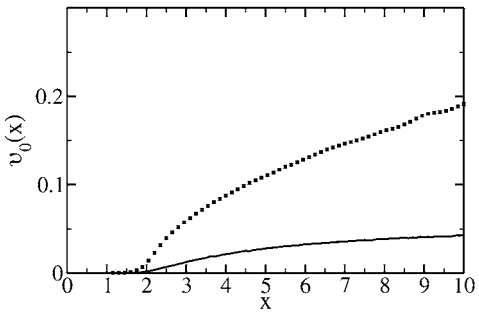

Figure 6. $\upsilon_0(x)$ from the numerically exact (squares) and the variational calculation (solid curve).

to resist a rigorous solution. If it could be solved then the calculation of $\upsilon_0(x)$ is reduced to the calculation of an integral over Ω_1 and Ω_2:

$$\upsilon_0(x) = -\tfrac{1}{3}\langle \boldsymbol{T}_{0n} \cdot \boldsymbol{f}_{0n}\rangle. \tag{43}$$

Therefore, we resort to an alternative. It is easy to prove (by the use of equation (9)) that (40) is the variational equation of the functional

$$\mathcal{F}[\boldsymbol{f}_{n_1n_2}(\Omega_1, \Omega_2)] = \tfrac{1}{3}[\langle \boldsymbol{f}_{n_1n_2} \cdot \mathcal{L}^{(2)\dagger} \boldsymbol{f}_{n_1n_2}\rangle - 2\langle \boldsymbol{T}_{n_1n_2} \cdot \boldsymbol{f}_{n_1n_2}\rangle]. \tag{44}$$

For a similar discussion see [38]. It can be easily shown by partial integration that

$$\langle \boldsymbol{f}_{n_1n_2} \cdot \mathcal{L}^{(2)\dagger} \boldsymbol{f}_{n_1n_2}\rangle = -\frac{1}{(4\pi)^2} \int \mathrm{d}\Omega_1 \int \mathrm{d}\Omega_2\, g^{(2)}_{n_1n_2}(\Omega_1, \Omega_2) \sum_{\alpha} [(\nabla_1 f^{\alpha}_{n_1n_2}(\Omega_1, \Omega_2))^2 + (\nabla_2 f^{\alpha}_{n_1n_2}(\Omega_1, \Omega_2))^2] \tag{45}$$

which is negative for all $\boldsymbol{f}_{n_1n_2} \neq$ constant, i.e. $\mathcal{L}^{(2)\dagger}$ is a negative operator. Therefore one can follow [38] and prove that the solution $\boldsymbol{f}^{\mathrm{sol}}_{n_1n_2}(\Omega_1, \Omega_2)$ of equation (40) is the non-degenerate maximum of $\mathcal{F}$. From equations (40), (43) and (44) we then find that

$$\upsilon_0(x) = \mathcal{F}[\boldsymbol{f}^{\mathrm{sol}}_{n_1n_2}(\Omega_1, \Omega_2)], \tag{46}$$

i.e. the maximum value of $\mathcal{F}$ is just $\upsilon_0(x)$. Since the maximum is non-degenerate the following inequality is true for any trial function $\boldsymbol{f}^{\mathrm{var}}_{n_1n_2}(\Omega_1, \Omega_2)$:

$$\upsilon_0^{\mathrm{var}}(x) \equiv \mathcal{F}[\boldsymbol{f}^{\mathrm{var}}_{n_1n_2}(\Omega_1, \Omega_2)] \leqslant \upsilon_0(x). \tag{47}$$

Choosing an appropriate trial function offers the possibility of determining a lower bound for $\upsilon_0(x)$ and therefore an upper bound for the critical length l_c.

The boundary value problem described above is similar to those arising from electrodynamics or hydrodynamics. Its singular part implies that $\boldsymbol{f}_{n_1n_2}(\Omega_1, \Omega_2)$ is discontinuous at the contact surface. This is similar to the behaviour of the electric field at a dipolar layer. Without restricting generality, we can choose $\boldsymbol{R}_{n_2} - \boldsymbol{R}_{n_1}$ along the z-axis. Then the relevant coordinate is $\phi = \phi_2 - \phi_1$ and contacts can occur at $\phi = 0^{\pm}$ or $\phi = \pi^{\pm}$ (see the discussion in section 2), i.e. $\boldsymbol{f}_{n_1n_2}(\Omega_{n_1}, \Omega_{n_2}) \equiv \boldsymbol{f}_{n_1n_2}(\theta_1, \theta_2, \phi_1, \phi)$ must be discontinuous at $\phi = 0$ and π. Next, equation (43) makes it obvious that $|\boldsymbol{T}_{n_1n_2} \cdot \boldsymbol{f}_{n_1n_2}|$ should be made as large as possible. This can be done by choosing $\boldsymbol{f}_{n_1n_2} \sim \boldsymbol{T}_{n_1n_2} \sim \boldsymbol{u}_1 \times \hat{\boldsymbol{r}}_{12}^{\perp} = (\cos\theta_1 \cos\phi_1, \cos\theta_1 \sin\phi_1, -\sin\theta_1)$. Finally, the calculation of $\mathcal{F}$ from equation (44) requires the calculation of the rhs of equation (45). Since $\nabla_i f^{\alpha}_{n_1n_2}(\Omega_1, \Omega_2)$ involves $1/\sin\theta_i$ for x- and y-components of the gradient, the integrals in equation (45) will not exist unless $f^{\alpha}_{n_1n_2} \sim (\sin\theta_1)^{\nu_1}(\sin\theta_2)^{\nu_2}$ with $\nu_1 \geqslant 1$ and $\nu_2 \geqslant 1$. These considerations suggest using the following trial function:

$$\boldsymbol{f}^{\mathrm{var}}_{n_1n_2}(\Omega_1, \Omega_2) \equiv \lambda \boldsymbol{h}^{\mathrm{var}}_{n_1n_2}(\Omega_1, \Omega_2) = \lambda \sin\theta_1 \sin\theta_2 \begin{pmatrix} \cos\theta_1 \cos\phi_1 \\ \cos\theta_1 \sin\phi_1 \\ -\sin\theta_1 \end{pmatrix} \times \begin{cases} \dfrac{\pi}{2} - (\phi_2 - \phi_1), & 0 < \phi_2 - \phi_1 < \pi \\ \dfrac{3\pi}{2} - (\phi_2 - \phi_1), & \pi < \phi_2 - \phi_1 < 2\pi \end{cases} \tag{48}$$

with λ being a variational parameter. For the $(\phi_2 - \phi_1)$-dependence we have made the simplest choice taking a linear variation with discontinuities at 0 and π. Note also that $\boldsymbol{f}^{\mathrm{var}}_{n_1n_2}(\Omega_1, \Omega_2)$ does not depend on either $\boldsymbol{R}_{n_2} - \boldsymbol{R}_{n_1}$ or $x = l/r_n$, which will be not true for the true, exact solution $\boldsymbol{f}^{\mathrm{sol}}_{n_1n_2}(\Omega_1, \Omega_2)$. Substituting $\boldsymbol{f}^{\mathrm{var}}_{n_1n_2}(\Omega_1, \Omega_2)$ into equation (44), where the first term is evaluated by equation (45), one obtains

$$\mathcal{F}[\boldsymbol{f}^{\mathrm{var}}_{n_1n_2}(\Omega_1, \Omega_2)] = F(\lambda) = \lambda^2 I_2 - 2\lambda I_1(x) \tag{49}$$

with

$$I_1(x) = \frac{1}{3}\frac{1}{(4\pi)^2} \int \mathrm{d}\Omega_1 \int \mathrm{d}\Omega_2\, \boldsymbol{h}^{\mathrm{var}}_{n_1n_2}(\Omega_1, \Omega_2) \cdot \boldsymbol{T}_{n_1n_2}(\Omega_1, \Omega_2) \tag{50}$$

$$I_2 = -\frac{1}{3}\frac{1}{(4\pi)^2} \int \mathrm{d}\Omega_1 \int \mathrm{d}\Omega_2 \sum_{\alpha} [(\nabla_1 h^{\mathrm{var},\alpha}_{n_1n_2}(\Omega_1, \Omega_2))^2 + (\nabla_2 h^{\mathrm{var},\alpha}_{n_1n_2}(\Omega_1, \Omega_2))^2]. \tag{51}$$

Note that I_2 does not depend on x. $F(\lambda)$ is easily maximized. As a result one obtains

$$\upsilon_0^{\mathrm{var}}(x) = F(\lambda_{\max}) = \frac{(I_1(x))^2}{(-I_2)}. \tag{52}$$

I_2 can be calculated analytically:

$$I_2 = -\tfrac{2}{81}(27 + 2\pi^2) \cong -1.154 \tag{53}$$

whereas $I_1(x)$ must be calculated by numerical integration, due to the non-trivial contact hypersurface. The result $\upsilon_0^{\mathrm{var}}(x)$ following from this approach is shown in figure 6. It is interesting that $\upsilon_0^{\mathrm{var}}(x)$ reproduces the crossover behaviour found for $\upsilon_0^{\mathrm{num}}(x)$ close to $x = 2$ from $\upsilon_0^{\mathrm{var}}(x) \approx 0$ for $x < 2$ to $\upsilon_0^{\mathrm{var}}(x) > 0$ for $x > 2$. Comparison of $\upsilon_0^{\mathrm{num}}(x)$ with $\upsilon_0^{\mathrm{var}}(x)$

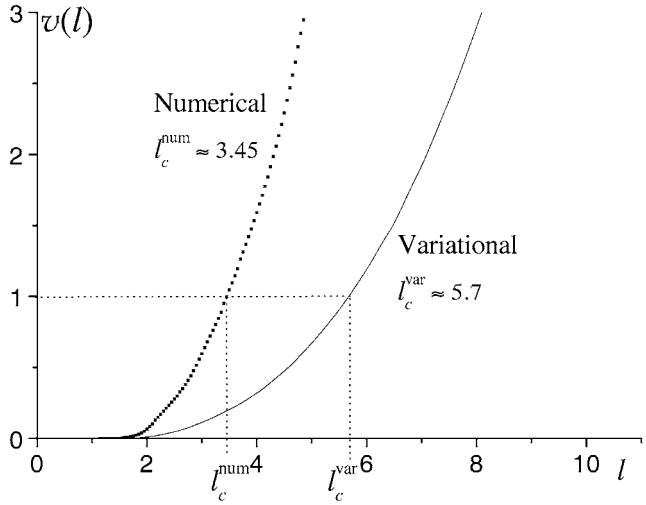

Figure 7. $\upsilon(l)$ for an sc lattice from the numerically exact (squares) and the variational calculation (solid curve). l_c denotes the critical length for which $\upsilon(l_c) = 1$.

confirms that $\upsilon_0^{\mathrm{var}}(x)$ is a lower bound for $\upsilon_0^{\mathrm{num}}(x)$, as it should be. Introducing $\upsilon_0(x)$ from both approaches into equation (36) leads to $\upsilon(l)$ represented in figure 7 for an sc lattice. From this figure we get

$$l_c^{\mathrm{num}} \cong 3.45, \qquad l_c^{\mathrm{var}} \cong 5.68 \qquad \text{sc lattice.}$$

$\upsilon(l)$ can be calculated for any periodic lattice. For the other cubic lattices we obtained

$$l_c^{\mathrm{num}} \cong \begin{cases} 2.78 \\ 2.20, \end{cases} \qquad l_c^{\mathrm{var}} \cong \begin{cases} 4.84 & \text{bcc lattice} \\ 3.96 & \text{fcc lattice.} \end{cases}$$

Since $\upsilon^{\mathrm{var}}(l) \leqslant \upsilon^{\mathrm{num}}(l) \cong \upsilon(l)$, it follows that $l_c^{\mathrm{var}} \geqslant l_c^{\mathrm{num}} \cong l_c$. The critical length decreases when going from sc to bcc to fcc lattice. This decrease is related to

(i) the increase of the coordination number z from six to eight to 12 and
(ii) a decrease of the nearest-neighbour distances r_1 from 1 to $\sqrt{3}/2$ to $\sqrt{2}/2$ (in units of the lattice constant a).

Since an increase of z and a decrease of r_1 results in an increase of the steric hindrance, l_c must decrease. As the increase of steric hindrance is equivalent to an increase of collisions, i.e. of contacts, our result has some similarity to that found in [39]. These authors have used a probabilistic approach in order to derive a criterion for the *mechanical* stability of an off-lattice system of infinitely thin hard rods in its randomly closed-packed glassy state. It has been found that a mechanically stable amorphous phase occurs if the average number of contact points per rod becomes five. However, such an arrangement of hard rods with $d = 0$ is dynamically unstable, as discussed in the introduction. In the simulation performed in [29] it was found that $l_c^{\mathrm{sim}} \cong 2.7$ for an fcc lattice. On the other hand [30] found $l_c^{\mathrm{sim}} \cong 4.5$ for an sc lattice. Note that in [30] the rods were fixed with one of their endpoints, and not with their centres. Our results for l_c^{num} and l_c^{var} agree satisfactorily with the simulational result of [29]. The difference between our result and that of [30] may be due to the different way of fixing rods on the lattice that was mentioned above.

The authors of [29] have also studied the l-dependence of the rotational diffusion constant $D(l)$ defined by

$$D(l) = \lim_{t\to\infty}\left(-\frac{1}{2t}\ln\left[\frac{1}{N}\sum_{n=1}^{N}\langle \boldsymbol{u}_n(t)\cdot\boldsymbol{u}_n(0)\rangle\right]\right). \tag{54}$$

The variation of D over about two orders in magnitude follows a power law $D(l) \sim (l_c - l)^{\gamma^{MD}}$ with $\gamma^{MD} \cong 4.2$. Since $\upsilon(l)$ is analytical for $l > 1$ it follows that $1-\upsilon(l) \sim l_c - l$ and therefore $D(l) \sim (l_c - l)$. Hence our analytical theory yields $\gamma = 1$ which differs significantly from γ^{MD}. This deviation may have two reasons. First, our result $\gamma = 1$ is mean-field-like (see, e.g., [22]). Note that in [22] going beyond the mean field approximation it has been found that $\gamma \cong 7/6$ [22] which is still close to one. Second, $\gamma^{MD} \cong 4.2$ is unusually high. Simulations and experiments of supercooled liquids usually yield $\gamma \approx 2$, consistent with most MCT analyses [14–16, 18–20].

4.2. Non-ergodicity parameter and dynamics close to l_c

The analysis in section 4.1 has proven that our theory predicts a dynamical glass transition at a critical length l_c. There are two important questions remaining. First, does the non-ergodicity parameter change at l_c in a continuous (type-A transition [14]) or discontinuous (type-B transition [14]) way? Second, what is the time or frequency dependence of the one-rod density $\rho_n^{(1)}$ close to l_c? The present section will give answers to both questions.

Let us expand $\hat{\rho}_n^{(1)}(\Omega; z)$ and $\hat{\boldsymbol{j}}_n^{(1)}(\Omega; z)$ into spherical harmonics:

$$\hat{\rho}_n^{(1)}(\Omega; z) = \sum_{\lambda}\hat{\rho}_{n,\lambda}^{(1)}(z)Y_\lambda(\Omega) \tag{55}$$

$$\hat{\boldsymbol{j}}_n^{(1)}(\Omega; z) = \sum_{\lambda}\hat{\boldsymbol{j}}_{n,\lambda}^{(1)}(z)Y_\lambda(\Omega) \tag{56}$$

where $\lambda = (j, m)$, $j = 0, 1, 2, \ldots, -j \leqslant m \leqslant j$. Furthermore, let us extend approximation (31) to finite z:

$$(\hat{\boldsymbol{D}}(\Omega_1, \Omega_2; z))^{\alpha\beta} \approx \hat{D}(z)\delta^{\alpha\beta}\delta(\Omega_1|\Omega_2). \tag{57}$$

It is easy to prove then that the Laplace transform of equations (15) and (21) leads to

$$\hat{\phi}_\lambda(z) \equiv \hat{\rho}_\lambda^{(1)}(z)/\rho_\lambda^{(1)}(t=0) = 1/[z + j(j+1)\hat{D}(z)], \tag{58}$$

where we skipped the index n.

The non-ergodicity parameter f_λ is defined as follows:

$$f_\lambda = \lim_{z\to 0} z\hat{\phi}_\lambda(z). \tag{59}$$

Taking into account approximation (57) we get from equation (24) after operating with $(1/4\pi)\int \mathrm{d}\Omega_1 \int \mathrm{d}\Omega_2$ on both sides the self-consistency equation for $\hat{D}(z)$:

$$\frac{1}{\hat{D}(z)} = \frac{1}{D_0} + \frac{1}{\hat{D}(z)}\hat{\upsilon}(\zeta; l), \qquad \zeta = z/\hat{D}(z), \tag{60}$$

with

$$\hat{\upsilon}(\zeta; l) = \tfrac{1}{3}\sum_n \langle \boldsymbol{T}_{0n}\cdot[\zeta - \mathcal{L}^{(2)\dagger}]^{-1}\boldsymbol{T}_{0n}\rangle. \tag{61}$$

Inverse Laplace transformation of equation (61) yields

$$\upsilon(t; l) = \tfrac{1}{3}\sum_n \langle \boldsymbol{T}_{0n}\cdot \mathrm{e}^{\mathcal{L}^{(2)\dagger}t}\boldsymbol{T}_{0n}\rangle. \tag{62}$$

Note that $\upsilon(t;l)$ is the time-dependent analogue of $\upsilon(l)$ defined in equation (33).

Equation (60) has a similar mathematical structure to the corresponding equation for a Lorentz gas obtained from a mode coupling approximation [40, 41]. Assuming that $\upsilon(t;l)$ does not decay more slowly than $t^{-5/2}$ for[6] $t \to \infty$ it follows from the Tauberian theorems [42] that

$$\hat{\upsilon}(\zeta;l) = \hat{\upsilon}(0;l) + \hat{\upsilon}'(0;l)\zeta + \mathrm{O}(\zeta^{3/2}) \tag{63}$$

where

$$\begin{aligned} &\hat{\upsilon}(0;l) \equiv \upsilon(l) \\ &\hat{\upsilon}'(0;l) = -\tfrac{1}{3}\sum_n \langle \boldsymbol{T}_{0n} \cdot (\mathcal{L}^{(2)\dagger})^{-2} \boldsymbol{T}_{0n} \rangle := -a(l) < 0. \end{aligned} \tag{64}$$

Substituting equations (63) and (64) into (60) and neglecting $\mathrm{O}(\zeta^{3/2})$ we get a quadratic equation for $z/\hat{D}(z)$, the physical solution of which is

$$z/\hat{D}(z) = \tfrac{1}{2}\left[\epsilon(l) + \sqrt{\epsilon^2(l) + z \cdot t_0}\right] \tag{65}$$

with

$$\epsilon(l) = \frac{\upsilon(l) - 1}{a(l_c)} = \begin{cases} < 0, & l < l_c \text{ (ergodic phase)} \\ \geqslant 0, & l \geqslant l_c \text{ (glass phase)} \end{cases} \tag{66}$$

and $t_0 = 4/(a(l_c)D_0)$ being a microscopic timescale. Note that equation (65) is identical to the corresponding equation obtained for the so-called F_1-model [14]. Accordingly, all results for the F_1-model [14] hold here as well. This implies

(i) that the glass transition is of type A, i.e. the non-ergodicity parameters (obtained from equations (58) and (59))

$$f_\lambda(l) = \begin{cases} 0, & l \leqslant l_c \\ \dfrac{\epsilon(l)}{j(j+1)} \cong \dfrac{\upsilon'(l_c)}{a(l_c)j(j+1)}(l - l_c), & l \to l_c^+ \end{cases} \tag{67}$$

vary continuously at l_c,

(ii) at the critical point $l = l_c$ and for $z \to 0$, $t \to \infty$

$$\hat{\phi}_\lambda(z) \cong \tfrac{1}{2}(zt_0)^{1/2}, \qquad \phi_\lambda(t) \cong \frac{1}{\sqrt{4\pi}}(t/t_0)^{-1/2} \tag{68}$$

and

(iii) for $|l - l_c| \ll 1$ and for $z \to 0$, $t \to \infty$

$$\hat{\phi}_\lambda(z,\epsilon) = (|\epsilon|/\omega_\epsilon)\hat{\phi}_\lambda(z/\omega_\epsilon), \qquad \phi_\lambda(t,\epsilon) = |\epsilon|\phi_\lambda(t/t_\epsilon) \tag{69}$$

with $\omega_\epsilon = t_\epsilon^{-1} = \epsilon^2/t_0$.

In other words, the (z,ϵ)- and (t,ϵ)-dependence follows from the master function $\hat{\phi}_\lambda$ and ϕ_λ (equation (68)), respectively, by use of the scaled frequency z/ω_ϵ and time t/t_ϵ. The timescale t_ϵ diverges as ϵ^{-2} when approaching the glass transition independent of the sign of ϵ.

[6] Our numerical result (figure 5) is consistent with this assumption. It is possible that the decay is exponential due to the compact configuration space of two needles in contrast to two hard spheres.

5. Summary and conclusions

Our main motivation has been the microscopic description of the glass transition for systems with trivial statics, i.e. systems which do not undergo an equilibrium phase transition to an ordered phase and do not have static correlations. For such systems, present microscopic theories like MCT and replica theory for structural glasses predict neither a dynamical nor a static glass transition. As a model we have chosen *N infinitely thin* hard rods with length L fixed with their centres on a periodic lattice with lattice constant a. The only relevant physical parameter is the dimensionless length $l = L/a$. Simulations for an fcc [29] and an sc lattice [30] strongly suggested that a *dynamical* glass transition occurs at a critical length $l_c^{\mathrm{sim}} \cong 2.7$ [29] and $l_c^{\mathrm{sim}} \cong 4.5$ [30]. Note that the rods in [30] were fixed at the lattice sites with one of their end points.

To describe the dynamics of our model we have used the generalized N-rod Smoluchowski equation from which we derived a hierarchy of coupled equations for $\delta\rho^{(k)}_{n_1\cdots n_k}(\Omega_1, \ldots, \Omega_k)$, the fluctuations of the reduced k-rod densities. Truncating at the second level and approximating the influence of surrounding rods on a pair of rods by the introduction of an effective diffusion tensor $\boldsymbol{D}$ we finally obtained a self-consistency equation for $\boldsymbol{D}$ (equation (25)). This equation describes a feedback mechanism (as MCT also does) which leads to a slowing down of the dynamics and ultimately to an orientational glass transition, similar to that occurring in plastic crystals [5–8, 11–13]. The model studied in the present paper may be applied to real plastic crystals as has been shown in [8].

One of the essential features of the present MCT for the glass transition is the cage effect [14]. For low temperature or high density an *extended* particle, e.g. a hard sphere, is captured in a cage. The occurrence of this cage is accompanied by the growth of *static* correlations. Particularly, the main peak of the static structure factor grows and this leads to an increase of the static vertices entering the MCT equations. If the vertices reach a critical strength the system will undergo a *dynamical* glass transition, provided ordering is prevented. In this sense the cage effect entering into MCT through the static correlations is of *static* nature. The model studied here does not have any static correlations, yet there is a cage effect. If the rods are long enough the tagged rod's motion can be strongly restricted to an 'orientational' cage (cf figure 2). This cage, however, is of pure *dynamical* nature and leads to a glass transition as well.

Comparing the results for the fcc lattice obtained from our theoretical framework with the additional approximation equation (31) with those from simulations [29, 30] one can say that both values $l_c^{\mathrm{num}} \cong 2.20$ and $l_c^{\mathrm{var}} \cong 3.96$ are in a reasonable range of $l_c^{\mathrm{sim}} \cong 2.7$ [29]. Taking into account that our approach involves uncontrollable approximations (equations (19) and (20)) this is a satisfactory result. The tendency of l_c to decrease when going from the sc lattice to the bcc to the fcc lattice is consistent with our expectation that l_c decreases with increase of the coordination number and decrease of the nearest-neighbour distances. Of course, second-, third- etc nearest neighbours also play a role, but with minor influence. Less satisfactory is the exponent, γ, of the power law, $D(l) \sim (l_c - l)^{\gamma}$, which is $\gamma = 1$, in contrast to $\gamma^{\mathrm{sim}} \cong 4.2$ [30]. Even if the simulated result turns out too high, the type-A transition result, $\gamma = 1$, cannot be the correct value. This requires an improvement of our microscopic approach. It is not obvious whether the approach presented in [22] which is based on rather qualitative arguments can serve as a guide.

It seems that the 'dynamical cage effect' leads to a discontinuous variation of the non-ergodicity parameter at l_c and is accompanied close to l_c by a two-step relaxation process, as can be seen from the orientational correlator studied in [29]. Such a two-step relaxation was first predicted by MCT [1, 14–16] and within this theory it is related to the cage effect. The present theoretical approach predicts a continuous transition for the glass order parameters f_λ.

Therefore it does not yield a two-step relaxation. This fact demands for an improvement of our theory, based on the hierarchy of equations for the k-rod densities. But on the other hand it is, of course, a big challenge to extend the present MCT such that it includes the *'dynamical cage effect'* described above and that a discontinuous glass transition occurs. If this turns out to be possible, it seems that the vertices must be generalized. Besides static correlations, i.e. correlators *at time* $t = 0$, they must also contain dynamical ones. These dynamical correlations may enter through a time-dependent force–force correlator $\int_0^\infty \mathrm{d}t \langle \boldsymbol{F}(t) \cdot \boldsymbol{F}(0) \rangle$, i.e. as a Laplace transformed correlator *at frequency* $z = 0$ (as found in the present approach). For systems with vanishing static correlations, as for our model, the vertices would be of purely dynamical nature. Now, increasing d to finite values will generate static correlations. For small thickness the 'dynamical cage' will be still dominant, but at a crossover value $d_{\mathrm{c.o.}}$ the static cage effect would become comparable with the dynamical one and for $d > d_{\mathrm{c.o.}}$ it would be the dominant one.

Let us come back to the choice of Brownian versus Newtonian dynamics. We have found that the glass transition is driven by the increase of the Laplace transform at $z = 0$ of the time-dependent torque–torque correlator of an isolated pair of rods. This correlator is different for Brownian and Newtonian dynamics. Therefore the critical length l_c will be not be the same for both dynamics. At present, it is not clear whether this is only a small effect. This is different from what has been found for liquids with non-trivial static correlations [33, 34]. However, the linear dependence of the nonergodicity parameters and of the diffusion constant on ϵ, the quadratic dependence of the frequency scale ω_ϵ on ϵ and the $t^{-1/2}$ dependence of the correlator at the critical length l_c should be independent of the type of dynamics.

It would be interesting to re-investigate the lattice model with infinitely thin hard rods by computer simulations. With present computers it should be possible to cover a larger time range and to study the dynamics close to l_c in greater detail. This would allow us to check whether the two scaling laws and other predictions of MCT are consistent with simulations. If the outcome of such a test proves consistency it would encourage theoretical efforts to extend the microscopic theory within the framework of MCT.

Besides rods on a lattice one could also investigate liquid systems of 'particles' built by crossing infinitely thin hard rods. If the number of 'legs' (rods) of a 'particle' becomes large they may exhibit quite similar dynamical behaviour to hard spheres, although there are no static correlations. The timescale on which these 'particles' realize that they are not hard spheres could be much larger than a typical timescale for structural relaxation.

To conclude, we have discussed a *purely dynamical* mechanism which also drives a glass transition and which up to now has received almost no attention. Its further investigation by computer simulations and analytical work seems to us a challenging task for the future.

Acknowledgments

We gratefully acknowledge a very fruitful and stimulating discussion with W Götze during the *Third Workshop on Non-Equilibrium Phenomena in Supercooled Fluids, Glasses and Amorphous Materials* in Pisa and his comments on the present manuscript. Helpful comments by M Fuchs and the preparation of most of the figures by D Garanin and M Ricker are gratefully acknowledged as well. GS acknowledges support from the National Science Foundation through grant no CHE 0111152 and the Alexander von Humboldt Foundation.

References

[1] Bengtzelius U, Götze W and Sjölander A 1984 *J. Phys. C: Solid State Phys.* **17** 5915
[2] Das S P and Mazenko G F 1986 *Phys. Rev.* A **34** 2265

[3] Mézard M and Parisi G 1996 *J. Phys. A: Math. Gen.* **29** 6515
Mézard M and Parisi G 1999 *Phys. Rev. Lett.* **82** 747
[4] Singh Y, Stoessel J P and Wolynes P G 1985 *Phys. Rev. Lett.* **54** 1059
[5] Suga H and Seki S 1974 *J. Non-Cryst. Solids* **16** 171
[6] Srinivasan A, Bermejo F J, de Andrés A, Dawidowski J, Zúñiga J and Criado A 1996 *Phys. Rev.* B **53** 8172
[7] Ramos M A, Vieira S, Bermejo F J, Dawidowski J, Fischer H E, Schober H, González M A, Loong C K and Price D L 1997 *Phys. Rev. Lett.* **78** 82
[8] Jiménez-Ruiz M, Criado A, Bermejo F J, Cuello G J, Trouw F R, Fernández-Perea R, Löwen H, Cabrillo C and Fischer H E 1999 *Phys. Rev. Lett.* **83** 2757
[9] Michel K H 1986 *Phys. Rev. Lett.* **57** 2188
Michel K H 1988 *Z. Phys.* B **71** 369
[10] Bostoen C and Michel K H 1991 *Phys. Rev.* B **43** 4415
[11] Criado A, Jiménez-Ruiz M, Cabrillo C, Bermejo F J, Fernández-Perea R, Fischer H E and Trouw F R 2000 *Phys. Rev.* B **61** 12082
[12] Affouard F, Cochin E, Decressain R and Descamps M 2001 *Europhys. Lett.* **53** 611
[13] Affouard F and Descamps M 2001 *Phys. Rev. Lett.* **87** 035501
[14] Götze W 1991 *Liquids, Freezing and the Glass Transition* ed J-P Hansen, D Levesque and J Zinn-Justin (Amsterdam: North-Holland) p 287
[15] Schilling R 1994 *Disorder Effects on Relaxational Processes* ed R Richert and A Blumen (Berlin: Springer) p 193
[16] Cummins H Z 1999 *J. Phys.: Condens. Matter* **11** A95
[17] Hansen J-P and McDonald I R 1986 *Theory of Simple Liquids* (London: Academic)
[18] Götze W and Sjögren L 1992 *Rep. Prog. Phys.* **55** 241
[19] Götze W 1999 *J. Phys.: Condens. Matter* **11** A1
[20] Kob W 1997 *Experimental and Theoretical Approaches to Supercooled Liquids: Advances and Novel Applications* ed J Fourkas, D Kivelson, U Mohanty and K Nelson (Washington, DC: American Chemical Society) p 28
[21] Kob W 1999 *J. Phys.: Condens. Matter* **11** R85
[22] Edwards S F and Vilgis Th 1986 *Phys. Scr.* T **13** 7
[23] Bergenholtz J and Fuchs M 1999 *Phys. Rev.* E **59** 5706
[24] Bergenholtz J and Fuchs M 1999 *J. Phys.: Condens. Matter* **11** 10171
[25] Bergenholtz J, Fuchs M and Voigtmann Th 2000 *J. Phys.: Condens. Matter* **12** 6575
[26] Szamel G 1993 *Phys. Rev. Lett.* **70** 3744
[27] Szamel G and Schweizer K 1994 *J. Chem. Phys.* **100** 3127
[28] Rubinstein M and Obukhov S P unpublished
[29] Renner C, Löwen H and Barrat J L 1995 *Phys. Rev.* E **52** 5091
[30] Obukhov S P, Kobsev D, Perchak D and Rubinstein M 1997 *J. Physique* I **7** 563
[31] Schilling R and Szamel G 2003 *Europhys. Lett.* **61** 207
[32] Cichocki B 1987 *Z. Phys.* B **66** 537
[33] Szamel G and Löwen H 1991 *Phys. Rev.* A **44** 8215
[34] Gleim T, Kob W and Binder K 1998 *Phys. Rev. Lett.* **81** 4404
[35] Cichocki B 1988 *Physica* A **148** 165
[36] Ackerson B J and Fleischman L 1982 *J. Chem. Phys.* **76** 2675
[37] Jones R B 1984 *J. Phys. A: Math. Gen.* **17** 2305
[38] Dhont J K G, van Bruggen P B and Briels W J 1999 *Macromolecules* **32** 3809
[39] Philipse A P and Verberkmoes A 1997 *Physica* A **235** 186
[40] Götze W, Leutheusser E and Yip S 1981 *Phys. Rev.* A **23** 2634
Götze W, Leutheusser E and Yip S *Phys. Rev.* A **24** 1008
[41] Götze W, Leutheusser E and Yip S 1982 *Phys. Rev.* A **25** 533
[42] Feller W 1971 *An Introduction to Probability Theory and its Applications* (New York: Wiley) p 442 ff